Published in IET Image Processing
Received on 31st July 2013
Revised on 18th October 2013
Accepted on 21st November 2013
doi: 10.1049/iet-ipr.2013.0565

ISSN 1751-9659

Diagnosis of diabetic retinopathy by employing image processing technique to detect exudates in retinal images

Sundararaj Wilfred Franklin[1], *Samuelnadar Edward Rajan*[2]

[1]*Department of Electronics and Communication Engineering, CSI Institute of Technology, Thovalai, Kanyakumari District, Nagercoil 629302, Tamilnadu, India*
[2]*Department of Electrical and Electronics Engineering, Mepco Schlenk Engineering College, Sivakasi 626005, Tamilnadu, India*
E-mail: swfranklin@rediffmail.com

Abstract: Diabetic retinopathy (DR) is a microvascular complication of long-term diabetes and it is the major cause of visual impairment because of changes in blood vessels of the retina. Major vision loss because of DR is highly preventable with regular screening and timely intervention at the earlier stages. The presence of exudates is one of the primitive signs of DR and the detection of these exudates is the first step in automated screening for DR. Hence, exudates detection becomes a significant diagnostic task, in which digital retinal imaging plays a vital role. In this study, the authors propose an algorithm to detect the presence of exudates automatically and this helps the ophthalmologists in the diagnosis and follow-up of DR. Exudates are normally detected by their high grey-level variations and they have used an artificial neural network to perform this task by applying colour, size, shape and texture as the features. The performance of the authors algorithm has been prospectively tested by using DIARETDB1 database and evaluated by comparing the results with the ground-truth images annotated by expert ophthalmologists. They have obtained illustrative results of mean sensitivity 96.3%, mean specificity 99.8%, using lesion-based evaluation criterion and achieved a classification accuracy of 99.7%.

1 Introduction

Diabetic retinopathy (DR) is a serious complication of diabetes and it is a rigorous and widespread eye disease which causes legal blindness and vision loss among the working age population. DR is the result of long-term diabetes and if detected and treated promptly in the early stage, visual loss can be prevented. The early stage of DR is characterised by its distinctive qualities such as irregularities and leakiness of blood vessels, but may progress to its severe form, which leads to blindness. Exudates are yellow-white lesions with relatively distinct margins and are lipid deposits present in the posterior pole of the fundus. DR is not painful and hence visual loss is often a late symptom, when treatment becomes less effective. If it is diagnosed at an early and still asymptomatic stage, laser photocoagulation is one of the effective treatments which prevent visual loss from macular oedema. For the early diagnosis of DR and to ensure that treatment is received on time, diabetic patients need to undergo regular screenings, in which retinal image analysis plays a major role [1, 2]. An automated exudates detection system becomes much useful to detect and treat DR at an early stage. Automated screening of DR makes use of non-mydriatic digital colour fundus cameras to capture the colour images of the retina [3], and these retinal images are examined to detect the presence of exudates.

Development of automated systems to detect DR from retinal images has received great importance from the research community [4, 5]. There are several ways in which image analysis helps to diagnose DR from colour fundus images of the human retina. One such contribution is image enhancement, by which the contrast and the sharpness of the images are improved to reduce noise. The other methods of image processing which help in the diagnosis of DR are detection and classification methods. Narasimha-Iyer *et al.* [6] used image enhancement technique by which the illumination component was estimated by using the normal retinal findings. Sopharak *et al.* [7] have proposed a technique to detect DR from fundus images automatically by using a set of optimally adjusted morphological operators and then by applying threshold operation. Sinthanayothin *et al.* [8] used a recursive region growing technique to detect the exudate region. Sanchez *et al.* [9] have proposed an algorithm based on Fisher's linear discriminant analysis. Yazid *et al.* [10] have applied an inverse surface thresholding technique for the automated detection of exudates from colour fundus images. Harangi *et al.* [11] have identified the regions containing exudates in retinal images by using greyscale

morphology and then active contour based method was used to extract the precise borders of the candidates. Akram *et al.* [12] have presented a new method that uses filter banks to extract the candidate regions and then applies a Bayesian classifier to detect the exudates and the non-exudates regions. Rocha *et al.*[13] have proposed a novel technique to identify exudates by constructing a visual word dictionary which represents the points of interest located within the regions that contain lesions associated with DR. Sinthanayothin *et al*. [14] and Osareh *et al*. [15] have applied standard contrast stretching techniques to enhance the image for further processing. Then, colour segmentation was performed by using fuzzy c-means (FCM) clustering algorithm. Walter [16] has proposed a new technique, in which certain selected features such as microaneurysms alone are enhanced. Cree *et al*. [17] have applied an image restoration technique for images of very poor quality. Peli and Peli [18] have also applied the image restoration technique and in this approach, the images were considered as sample functions of stochastic process. Hsu *et al*. [19] have proposed a technique to find the normal and the abnormal areas of the retinal images by using intensity properties for dynamic clustering. A technique was proposed by Walter *et al.* [20], in which the exudates were detected by using their high-greylevel variation and morphological reconstruction techniques were employed to determine the exact contours. Sánchez *et al*. [21] have proposed an automatic method, which is a lesion associated with DR. A new technique was proposed by Zhang and Chutatape [22], in which fuzzy c-means clustering was used to detect the abnormal regions. Osareh *et al*. [23] used fuzzy c-means clustering with Gaussian smoothed histograms to detect the hard exudates. Li and Chutatape [24] have used region growing technique by combining canny edge detection to segment the exudates regions from the fundus images. Wang *et al*. [25] proposed an effective approach to detect the presence of the exudates by combining the brightness adjustment procedure with the statistical classification method and the local-window-based verification strategy.

2 Methodology

This research paper proposes a new effective technique for the detection of exudates in the retinal images by using artificial neural network. The most prevalent earliest sign of diabetic macular oedema is associated with the presence of exudates within the macular region. Hence, the task of detecting exudates by using computer-based analysis plays a vital role in the diagnosis of DR [26]. These exudates have high-grey-level variation from its surrounding background and hence they are much visible as bright patterns in colour fundus images [27]. The technique proposed in our work identifies the portion of the retinal images that contain exudates and separates them from other retinal pathologies. These retinal blood vessel irregularities were identified by using a multilayer perceptron neural network for which the inputs were derived from colour, size, edge strength and texture features. This exudates detection technique helps to examine whether DR is present or not.

2.1 Image database

The retinal images used to test and evaluate the performance of our system were taken from the DR database DIARETDB1. It acts as an essential tool for reliable assessments and comparisons of exudates detection algorithms. The DIARETDB1 database consists of eighty nine high quality colour fundus images, of which 84 images contain atleast mild signs of DR including exudates and the remaining five images are of healthy retinas, which do not contain any sign of DR. The images were captured in the Kuopio University hospital. Even though the abnormalities present in the database are quite small, they appear close to the macula which threatens the eyesight. These retinal images available in the database were acquired by using a digital fundus camera with a 50° field-of-view (FOV). The images were captured with different image settings such as flash intensity, shutter speed, aperture and gain. This database is widely used as a practical tool to evaluate the performance of various diagnostic techniques without performing any calibration. This dataset also contains expert ophthalmologist's annotated ground truth images which can be compared with the computer generated DR findings to ensure its accuracy. The ground truth contains all the description of visual appearance of the DR findings. The images used for evaluating this procedure have not been recompressed or altered after its reception from the database. Our proposed algorithm has been tested with the retinal images available in this database as input to our system and has produced significant output, which is consistent with the ground truth.

2.2 Preprocessing

Initially, the retinal images which have to be analysed for DR must undergo preprocessing. The few abnormalities present in the retinal fundus images are very small in size and hence their detection becomes quite confused because of the presence of noise. The important objective of image preprocessing is to remove noise and to seclude the dark abnormalities from the exudates regions, which appear as bright lesions in the retinal images. The colour fundus image in which each pixel has the three primary colour components red, green and blue was initially given as input to the system. In preprocessing, first the original fundus image that uses the red, green and blue (RGB) colour space was transformed into Lab colour space. This transformation prevents the problems associated with the application of grey scale methods to each of the components because of the high correlation between these components. Next, replace the luminosity layer with the processed data and then convert the images back to the original colour space and apply mean filtering. A few examples of the retinal images given as input to the multilayer perceptron neural network can be seen in Fig. 1.

2.3 Contrast enhancement

Originally, the retinal images captured by using fundus cameras might be of low contrast and with non-uniform illumination and their contrast must be enhanced before using them for exudates detection [28]. Hence, to enhance the contrast of these retinal images, contrast limited adaptive histogram equalisation, which operates over small regions in the image called tiles, was applied. It computes many histograms, each corresponds to an individual fragment of the retinal image and then it applies them to redistribute the intensity values of the image. Hence, it becomes significant to enhance the local contrast of the image and thereby gives detailed information of the exudates present in the fundus image. The contrast of these

doi: 10.1049/iet-ipr.2013.0565

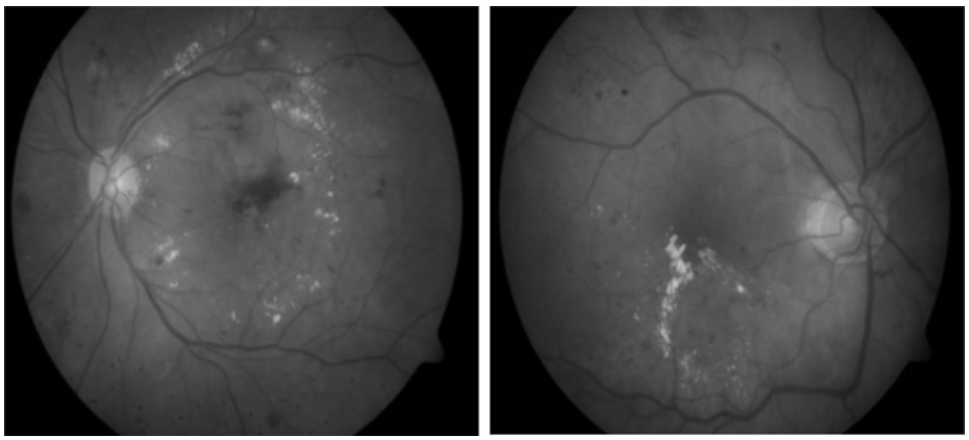

Fig. 1 *Retinal images containing exudates, given as input to the multilayer perceptron neural network*

regions was improved by transforming each pixel by using a transformation function which is proportional to the cumulative distribution function of the pixels in the neighbourhood region. Consider an image $\{x\}$ where n_i is the number of occurrences of the grey level i. The probability of occurrence of a pixel of level i in the image is given by

$$p_x(i) = p(x = i) = \frac{n_i}{n}, \quad 0 \le i < L \tag{1}$$

where L is the total number of grey levels in the image, n is the total number of pixels in the image and $p_x(i)$ is the histogram of the image for pixel value i, normalised to [0, 1].

The cumulative distribution function corresponding to p_x is given by

$$\mathrm{cdf}_x(i) = \sum_{j=0}^{i} p_x(j) \tag{2}$$

which is also the accumulated normalised histogram of the image. A transformation of the form $y = T(x)$ is created to produce a new image $\{y\}$, such that its cumulative distribution function will be linearised across the value range, that is

$$\mathrm{cdf}_y(i) = iK \tag{3}$$

for some constant K. Contrast limited adaptive histogram equalisation technique was applied to improve the contrast of the image and also to enhance the separability between the exudates and the background in the retinal images. It also makes the hidden features of the retinal images more visible by smoothing the distribution of the used grey values.

2.4 Feature extraction and learning

To classify the image into candidate regions of exudates or non-exudates classes, it must be represented by using significant features to achieve the best class separability. To select an adequate set of features, we paid careful attention to the characteristics that ophthalmologists use to distinguish exudates from other retinal lesions or structures. In our method, the candidate regions were classified by using various features such as colour, size, shape, edge strength and texture. We have examined with different colour spaces such as RGB, HIS and Luv, and found that Luv colour space that separates the luminance and the chrominance values was more appropriate. Luv colour space is designed in such a way that it completely separates the grey-scale intensity from the colour components of an image. A few important properties of Luv colour space are its device-independency and perceptual linearity. Also, Luv colour space is used to improve the perceptual values where the differences scale better with the capability of perceiving distinctive tones. Luv colour space is superior in perceptual uniformity and provides excellent estimates of colour difference between two colour vectors. Hence, Luv colour space is enormously applied in image processing systems, where the exact perceptual reproduction of colour images across the entire system is of primary importance. Hence, it is more appropriate to make use of Luv colour space and hence we chose it.

Among a number of feasible features, we have chosen fifteen visually distinctive features to classify the candidate regions as exudates and non-exudates region. It includes, mean Luv value inside the region (1–3), standard deviation of Luv value inside the region (4–6), mean Luv value outside the region that belongs to a rectangular area around the region of five pixels distance (7–9), standard deviation of Luv value outside the region that belongs to a rectangular area around the region of five pixels distance (10–12), region size (13), region edge strength (14) and region compactness (15). These feature sets were applied as inputs to the neural network.

Region size was calculated as the number of pixels inside the region and region edge strength was calculated as an average of the edge values in the perimeter of the region. Region compactness is the ratio between the square of the perimeter and the area of the region, both measured in terms of number of pixels. The compactness value, M, can be calculated by using the formula

$$M = 4\Pi\left(\frac{\text{area}}{\text{perimeter}^2}\right) \tag{4}$$

where area is the number of pixels in a specific region and perimeter is the total number of pixels around the boundary of each region.

The edge values were obtained by applying the canny method which detects the edges by calculating the local maxima of the gradient of I. It was calculated by using the

derivative in the horizontal direction (G_x) and the vertical direction (G_y) as

$$G = \sqrt{G_x^2 + G_y^2} \tag{5}$$

where G is the edge gradient. The direction can be determined as

$$\Theta = \arctan\left(\frac{G_y}{G_x}\right) \tag{6}$$

This method exploits two thresholds namely high and low thresholds to detect the strong and the weak edges. In our method, only if the weak edges are connected to the strong edges, they may be incorporated in the output. This method applies a high threshold to the gradient for low edge sensitivity and a low threshold for high edge sensitivity. Hence, this method becomes more efficient for the prediction of the weak edges.

Also, to extract the valuable texture features in the retinal fundus images, we have applied a set of Gabor filters with different frequencies and orientations. To locate the exudates in the retinal images, we have used a Gabor filter bank arranged in 16 different orientations. Mathematically, a two-dimensional (2D) Gabor function, g, is the product of a 2D Gaussian and a complex exponential function and is given by

$$g_{\theta,\lambda,\sigma_1,\sigma_2}(x, y) = \exp\left\{-\frac{1}{2}M(x, y)^{\mathrm{T}}\right\} \times \exp\left\{\frac{j\Pi}{\lambda}(x\cos\theta + y\sin\theta)\right\} \tag{7}$$

where $M = \mathrm{diag}(\sigma_1^{-2}, \sigma_2^{-2})$. The parameter θ represents the filter orientation, λ represents the filter wavelength which modifies the sensitivity to high or low frequencies, σ_1 and σ_2 characterise the filter standard which represents the scale value at orthogonal directions. To optimally choose the parameters of a Gabor filter, an unsupervised approach, in which, a filter bank which spreads throughout the frequency plane was used. To tune the Gabor filter response to specific pattern such as exudates, it becomes necessary to adjust the Gabor filter bank parameters, namely orientations, frequencies or wavelengths and scales appropriately.

Each pixel in the retinal image was classified as exudates or non-exudates, by using a multilayer perceptron neural network. In our method, a multilayer feed forward network which uses extended gradient-descent-based delta learning rule, commonly known as back propagation rule was employed. Back propagation is an efficient method for training the multilayer artificial neural network. Back propagation provides a well-organised technique to modify the weights in a feed forward network, with differentiable activation function units, to learn a training set of input–output examples. The number of layers in the feed forward network is represented as n, and L_i represents the number of neurons in the ith layer, and the total number of weights is given by

$$N = \sum_{i=1}^{n-1} L_i L_{i+1} \quad \text{where} \quad i = 1, 2, \ldots, n \tag{8}$$

The learning capacity, C, is an important parameter which determines how much ability a system has to learn. For a three layer network, the learning capacity is bounded by

$$\frac{nh}{\log(nh^2)} < C < nh\log(h) \tag{9}$$

where h is the number of hidden nodes and n is the number of input nodes.

The neural network trained for the final classification must have input nodes that correspond to the size of the feature vector selected. The neural network applied in our method was a three layer perceptron having 15 input nodes, one hidden layer with an optimum number of around 20 hidden neurons and a single output node. The final classification of the pixels as exudates or non-exudates was achieved by this single output node, as shown in Fig. 2.

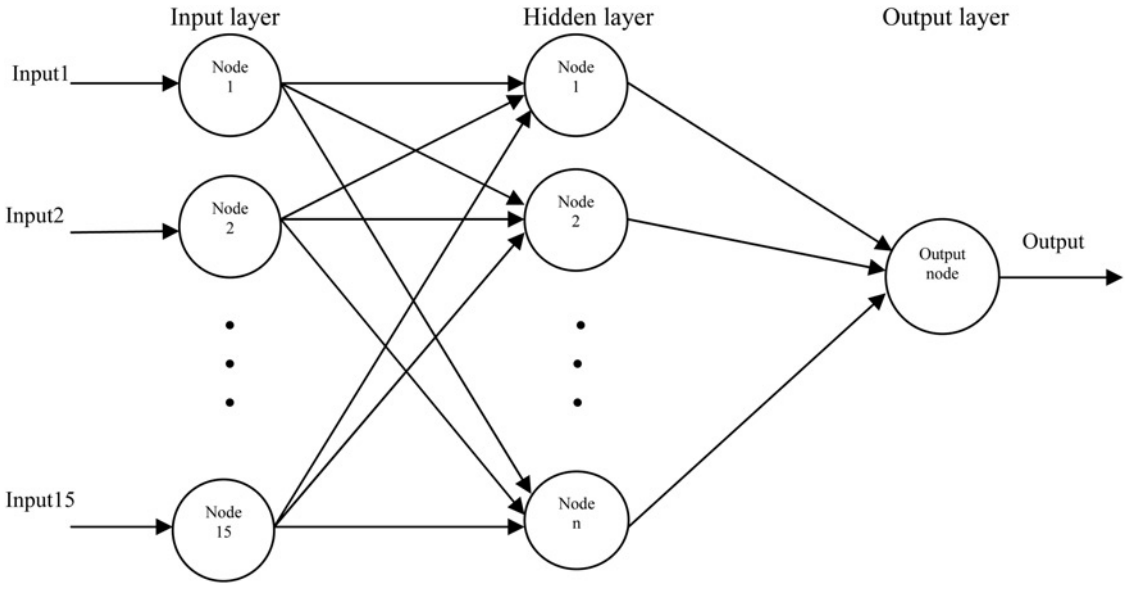

Fig. 2 *Three-layer feed forward neural network diagram, used for exudates detection*

doi: 10.1049/iet-ipr.2013.0565

2.5 Classification

In this phase, our proposed algorithm performs the classification of the pixels between the two classes, exudates and non-exudates. To classify the pixels into the exudates or the non-exudates classes, we have represented those using relevant and significant features that produced the best class separability. By making use of features such as colour, size, shape, edge strength and texture, the segmented regions were obviously discriminated as exudates or non-exudates regions. These features are used to characterise each of the possible candidate pixels to determine its type as exudates or non-exudates. Clinically, ophthalmologists use colour information to differentiate various pathological conditions. Similarly, coloured objects such as exudates are differentiated with these additional features of size, shape, edge and texture. A significant means for describing an exudates or non-exudates region is to score quantitatively the content of texture of that region. The elements used to express the texture feature consist of coarseness, contrast and directionality. Coarseness illustrates the rough degree of texture, contrast means the pitch distribution of brightness and directionality expresses the specific direction of the texture. The feature set has been selected properly to maximise the between-class discrimination while minimising the within-class discrimination. The selected feature set must be as small as possible to overcome the annoyance of dimensionality and so we have selected 15 features among the discriminative attributes of a much larger set. During classification, features that provide colour information have contributed drastically much than the other features.

This classification was performed by using the different training sets extracted from each colour fundus image. To diagnose the presence of DR, screening has to be performed on a large number of retinal images and it becomes significant that the classification is time efficient and precise [29]. Considering all these constraints, neural network using back propagation algorithm was applied. The neural network performs the following tasks for each training pair. At the first stage which is the initialisation of the weights, a few small random variables are assigned. In the next stage, named as feed forward stage, each input unit (X_i) receives an input signal (x_i) and transmits this signal to all the units to the layer above, that is, hidden units, $z_1, \ldots, z_p$. Each hidden unit then calculates the activation function

$$Z_j = f\left(z_{inj}\right) \tag{10}$$

where

$$z_{-inj} = v_{oj} + \sum_{i=1}^{n} x_i v_{ij} \tag{11}$$

v_{oj} is the bias on hidden unit j, v_{ij} is the interconnection weight between the input layer and the hidden layer and the activation function f is an arbitrary function. Each hidden unit sends this signal to its output unit.

Each output unit (y_k, $k = 1, \ldots, m$) then sums its weighted input signals from the hidden layer and then applies its activation function Y_k to calculate the output signals

$$Y_k = f\left(y_{-\text{ink}}\right) \tag{12}$$

where

$$y_{-ink} = w_{ok} + \sum_{j=1}^{p} z_j w_{jk} \tag{13}$$

w_{ok} is the bias on the output unit k, and w_{jk} is the interconnection weight between the hidden layer and the output layer.

During the back propagation of the errors, each output unit y_k compares its calculated activation with its target value t_k to find out the related errors for that pattern with that unit. The error information term at the output unit δ_k is given as

$$\delta_k = \left(t_k - y_k\right) f'\left(y_{-ink}\right) \tag{14}$$

It is used to distribute the error at the output unit y_k back to all the units in the previous layer. Then, each hidden unit (z_j, $j = 1, \ldots, n$) sums its delta inputs from the units in the above layer as

$$\delta_{-inj} = \sum_{k=1}^{m} \delta_k w_{jk} \tag{15}$$

also the error information term

$$\delta_j = \delta_{-inj} f'\left(z_{-inj}\right) \tag{16}$$

is computed for each hidden unit. During the final stage, the weights and the bias are updated by using the δ factor and the activation, by using α as the learning rate. Each output unit updates its weights and the bias by using the weight correction term ΔW_{jk} and the bias correction term ΔW_{ok}, where $\Delta W_{jk} = \alpha \delta_k z_j$ and

$$\Delta W_{ok} = \alpha \delta_k \tag{17}$$

therefore W_{jk} (new) = W_{jk} (old) + ΔW_{jk} and

$$W_{ok}\ (\text{new}) = W_{ok}\ (\text{old}) + \Delta W_{ok} \tag{18}$$

Also, the weights and the bias are updated for each hidden unit. Finally, the stopping condition was tested, where the stopping condition may be a minimisation of the errors, the number of epochs and so on. The idea we have used to avoid overfitting is to prevent co-adaptation of the hidden units. The prime concept is to take a large model that overfits easily and sample repetitively and train smaller sub-models from it. Subsequently, all the sub-models share parameters from the large model, and hence this procedure trains the large model which is then used at the time of testing. This idea is applied independently for each hidden unit and for each training case. We have demonstrated this concept and found that it works properly in feed forward neural networks. Also, an effective approach to avoid overfitting is early stopping. The results obtained by detecting the candidate exudates regions superimposed on the original fundus images after performing the classification task are shown in Fig. 3.

The most important attribute that makes the neural networks more powerful in exudates detection is its competence to exploit non-linear classification boundaries attained during training of the network. The other elegant feature of the neural network is its ability to learn. With

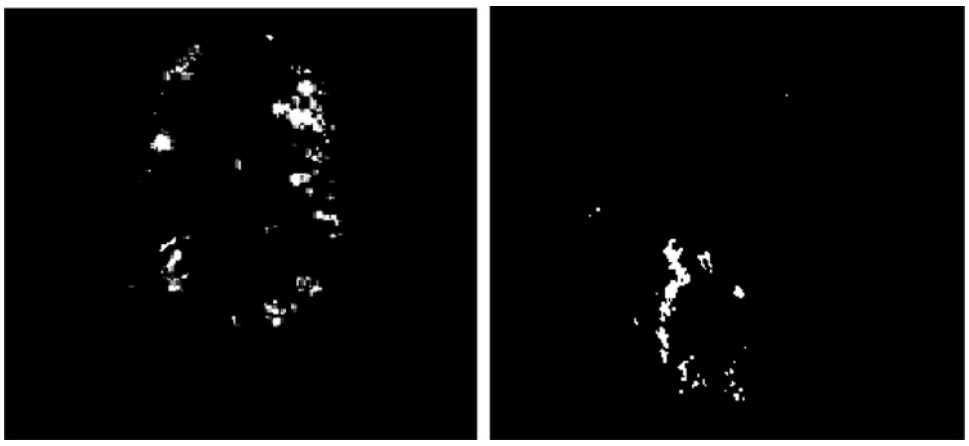

Fig. 3 *Classification of the pixels as exudates, after optic disc elimination*

appropriate selection of a fine training set which consists of all potential features, the network can learn the classification boundaries in its feature space.

This neural network classifier has been selected for pixel classification as the exudates or the non-exudates only after proper method accuracy assessment. The experimentation carried out to evaluate the effectiveness of this system proves its capability to render accurate results. The neural network classifier demonstrated better performance and based on the illustrative results obtained, it is clear that the neural network is appropriate for the classification of the pixels as exudates or non-exudates. The training set robustness revealed by this neural network based method permits its automated application to images captured under diverse conditions. In this regard, we state that our proposed method, in its different stages such as preprocessing, feature extraction and classification use a set of parameters unchanged to afford the best accuracy on the test images.

3 Results

We have tested and evaluated our proposed algorithm prospectively by using the retinal images of the DIARETDB1 Database. This technique proves itself to be one of the valuable tools for the diagnosis of DR, by detecting the presence of hard exudates in the retinal images. We have composed the learning and the test sets by using 57 colour retinal images taken from the database we have used, which contains 5137 objects for training and testing the neural network. These objects were labelled as exudates or non-exudates by an ophthalmologist to obtain a fully labelled dataset. We have split the dataset randomly into 78% for training and 22% for testing and hence the training set has 4010 candidates, of which 2107 were labelled as exudates. The remaining 1127 candidates, of which 476 were labelled as exudates were used as testing set. We have used a 10-fold cross validation with the training and the validation data. Illustrative exudates detection results for a few fundus images from DIARETDB1 are shown in Fig. 4.

The results obtained after the exudates detection were superimposed on the original image and thereby the indistinct exudates regions were visibly enhanced. Thus, it facilitates the ophthalmologists to observe the exudates regions more apparently and to diagnose the pathology more quickly. This algorithm has been tested and evaluated to determine its ability to distinguish between normal retinal images and images which contain exudates. The algorithm has exactly identified the presence of the exudates and on the other hand it did not misclassify any exudates from the healthy retinas. To measure the accuracy of our algorithm, we have computed the sensitivity, the specificity and the predictive value and this evaluation mechanism proves how precisely it detects the exudates in the retinal images. Sensitivity is the percentage of the abnormal fundus

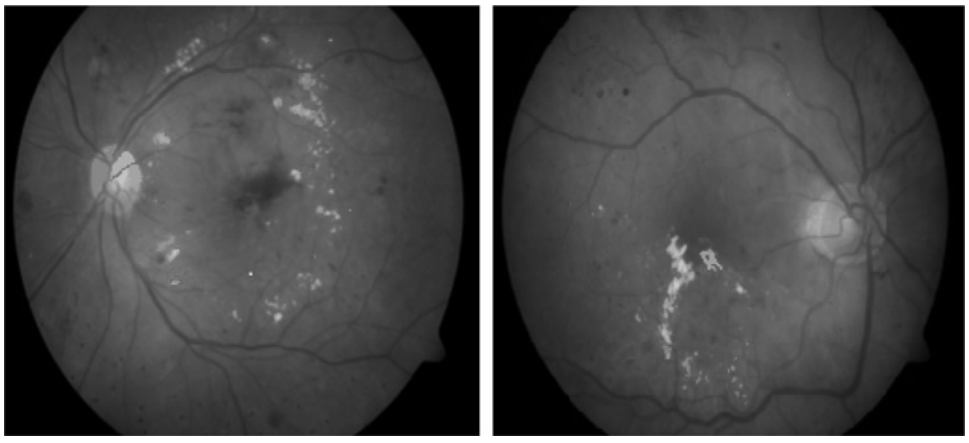

Fig. 4 *Final classification result of this exudates detection technique by using artificial neural network*

doi: 10.1049/iet-ipr.2013.0565

Table 1 Results obtained after the classification of the pixels as exudates and non-exudates

Images	TP	FP	TN	FN	Sensitivity	Specificity	Predictive value	Accuracy
1	1834	124	165263	36	98.07	99.92	93.66	99.90
2	1128	142	173407	41	96.49	99.91	88.82	99.89
3	2291	126	137136	134	94.47	99.90	94.79	99.81
4	6899	128	168685	42	99.39	99.92	98.17	99.90
5	2296	58	12594	24	98.96	99.54	97.53	99.45
6	3121	172	133576	162	95.06	99.87	94.77	99.76
7	5467	165	120611	294	94.89	99.86	97.07	99.64
8	2964	285	110394	74	97.56	99.74	91.22	99.68
9	2312	467	100208	98	95.93	99.54	83.19	99.45
10	1721	135	136052	54	96.95	99.90	92.73	99.86
11	2382	154	152321	151	94.03	99.89	93.92	99.80
12	3619	204	173693	217	94.34	99.88	94.66	99.76
13	3476	87	198754	152	95.81	99.95	97.56	99.88
14	2528	104	11507	68	97.38	99.10	96.04	98.79
15	2893	273	149827	149	95.10	99.81	91.38	99.72

classified as abnormal itself by applying the detection technique. Specificity is the percentage of the normal fundus classified as normal itself by using this detection technique. To compute the sensitivity, the specificity, the predictive value and the accuracy of this method, four quantities namely true positive (TP), false positive (FP), false negative (FN) and true negative (TN) were used. TP is the number of exudates pixels properly detected as exudates pixels. FP is the number of non-exudates pixels wrongly detected as exudates pixels. FN is the number of exudates pixels wrongly detected as non-exudates pixels, that is, exudates pixels that were not detected. TN is the number of non-exudates pixels properly detected as the non-exudates pixels itself. Sensitivity and specificity were computed by making use of these four quantities as

$$\text{Sensitivity} = \frac{\text{TP}}{\text{TP} + \text{FN}} \tag{19}$$

$$\text{Specificity} = \frac{\text{TN}}{\text{TN} + \text{FP}} \tag{20}$$

Also, predictive value was calculated, which is the probability of the pixels that have been classified as exudates are really exudates themselves

$$\text{Predictive value} = \frac{\text{TP}}{\text{TP} + \text{FP}} \tag{21}$$

The classification accuracy of this method was calculated by using the formula

$$\text{Accuracy} = \frac{\text{TP} + \text{TN}}{\text{TP} + \text{FP} + \text{TN} + \text{FN}} \tag{22}$$

To exhibit the performance of our method, we have presented the classification results obtained in Table 1.

Table 1 summarises the quantitative results of TP, FP, TN, FN, sensitivity, specificity and the predictive value obtained on the test set for the neural network configuration used in our method. We have obtained a mean sensitivity of 96.3%, mean specificity of 99.8% and a predictive value of 93.7%, by using lesion-based criterion and also obtained a classification accuracy of 99.7%.

3.1 Performance evaluation

The images of the DIARETDB1 database were of variable characteristics and it was very much useful to examine the performance of our method and thus it becomes suitable for its usage in the clinical environment. We have tested our algorithm by using the retinal images of diabetic patients which contain exudates and other lesions such as haemorrhages, microaneurysms and cotton wool spots. Our algorithm perfectly identified and effectively detected the presence of exudates by confiscating other yellow lesions. The performance of our method was evaluated quantitatively in terms of lesion-based criterion by comparing our results with the ophthalmologist's ground-truth images. Thus, it facilitates to compare the resulting extractions and to achieve quantitative evaluation. In the evaluation part, if the sensitivity and the specificity values obtained are higher, then the screening method is considered to be better, and it is achieved in our method.

Fig. 5 shows the receiver operating characteristic (ROC) curve for the detection of the exudates in the retinal images. A point of the ROC curve that has a high specificity value can be used to reduce the amount of false positives in the classification phase of our method. This method proves itself to be more efficient in detecting the presence of the exudates in the colour fundus images. The sensitivity and the specificity values obtained by our algorithm were very

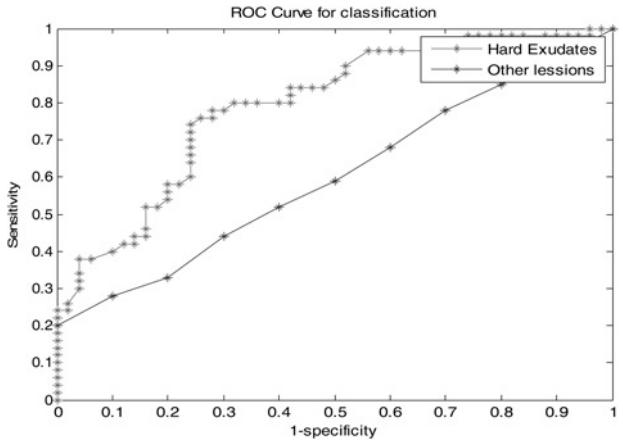

Fig. 5 *ROC curve for the classification of the exudates*

high and hence we state that our algorithm does not misclassify a non-exudates pixel as an exudates pixel. Our algorithm was assessed to determine its ability to recognise the difference between the images of the healthy retinas and the retinal images which contain lesions such as exudates. We have observed that our algorithm precisely detected all the retinal images which have exudates and also it has not detected any exudates from the normal retinal images. These results manifest the accuracy of our method and prove it to be the best one.

4 Conclusions

An efficient algorithm for the detection and segmentation of the exudates from the retinal images, which plays an important role in the diagnosis of DR has been presented in this paper. In this work, we have investigated and presented a novel technique which automatically detects the exudates from the DR patients retinal images. Colour information was used in the preprocessing stage of our algorithm and thereby better performance was achieved in the image segmentation stage. It is considered to be an important feature to distinguish different lesions present in the colour fundus images.

The detection of exudates by employing neural network implemented in this research work has a computationally demanding training phase. It also ensures a proficient classification phase, which classifies each pixel as exudates or non-exudates pixel and has proven excellent presentation. It is proved that the performance of the network increases with the progressive increased number of randomly selected training samples. Based on the results, it is seen that if the number of hidden layers increases, the convergence becomes slower and the training becomes tiresome. It is also observed that, increasing the number of hidden layers requires a larger learning rate and if the learning rate becomes too high, it may result in oscillations. Proper selection of the training set is also a prime factor which validates the performance of the algorithm. Our work engrosses using different training sets extracted automatically for each image which endures the large inter-image variability. Based on the literature, it is recommended by the British Diabetic Association that a system which can achieve sensitivity of 80% or above and a specificity of 95% or above can maximise cost-effectiveness in screening of DR. Our method has obtained very high sensitivity and specificity values and hence, it is best suited for the screening of DR. Owing to the presence of artefacts that have similar characteristics like exudates, very few false detections of exudates were observed in our evaluation procedure.

This screening system is conceptually quite easier and hence it can be implemented very effectively even with a low configuration computing system. This system will be incredibly useful in developing countries, where the availability of ophthalmologists is inadequate to treat more DR patients, thereby significantly reducing their workload. Ophthalmologists can make use of this system as a preliminary diagnosis tool in their DR screening procedure, which helps them to diagnose the symptom more accurately and quickly. In addition to this exudates detection, inclusion of retinal blood vessel segmentation can facilitate ophthalmologists to make earlier decisions on laser treatment. Also, including effective microaneurysm and haemorrhage detection technique along with this system can improve its ability to validate the degree of DR. The results obtained while evaluating our system proves itself that computer-based retinal image analysis is the most powerful tool to detect exudates and diagnose DR easily in the early stages.

5 References

1 Patton, N., Aslam, T.M., MacGillivray, T., *et al.*: 'Retinal image analysis: concepts, applications and potential', *Prog. Retin. Eye Res.*, 2006, **25**, (1), pp. 99–127

2 Bresnick, G.H., Mukamel, D.B., Dickinson, J.C., Cole, D.R.: 'A screening approach to the surveillance of patients with diabetes for the presence of vision-threatening retinopathy', *Ophthalmology*, 2000, **107**, (1), pp. 19–24

3 Niemeijer, M., Ginneken, B.V., Cree, M.J., *et al.*: 'Retinopathy online challenge: automatic detection of microaneurysms in digital color fundus photographs', *IEEE Trans. Med. Imaging*, 2010, **29**, (1), pp. 185–195

4 Philip, S., Fleming, A.D., Goatman, K.A., *et al.*: 'The efficacy of automated 'disease/no disease' grading for diabetic retinopathy in a systematic screening programme', *Br. J. Ophthalmol.*, 2007, **91**, (11), pp. 1512–1517

5 Abràmoff, M.D., Niemeijer, M., Suttorp-Schulten, M.S.A., Viergever, M.A., Russell, S.R., Ginneken, B.: 'Evaluation of a system for automatic detection of diabetic retinopathy from color fundus photographs in a large population of patients with diabetes', *Diabetes Care*, 2008, **31**, (2), pp. 193–198

6 Narasimha-Iyer, H., Can, A., Roysam, B., *et al.*: 'Robust detection and classification of longitudinal changes in color retinal fundus images for monitoring diabetic retinopathy', *IEEE Trans. Biomed. Eng.*, 2006, **53**, (6), pp. 1084–1098

7 Sopharak, A., Uyyanonvara, B., Barmanb, S., Williamson, T.H.: 'Automatic detection of diabetic retinopathy exudates from non-dilated retinal images using mathematical morphology methods', *Comput. Med. Imaging Graph.*, 2008, **32**, (8), pp. 720–727

8 Sinthanayothin, C., Boyce, J.F., Williamson, T.H., *et al.*: 'Automated detection of diabetic retinopathy on digital fundus images', *Diabet. Med.*, 2002, **19**, (2), pp. 105–112

9 Sánchez, C.I., Hornero, R., López, M.I., Aboy, M., Poza, J., Abásolo, D.: 'A novel automatic image processing algorithm for detection of hard exudates based on retinal image analysis', *Med. Eng. Phys.*, 2008, **30**, (3), pp. 350–357

10 Yazid, H., Arof, H., Isa, H.M.: 'Automated identification of exudates and optic disc based on inverse surface thresholding', *J. Med. Syst.*, 2012, **36**, pp. 1997–2004

11 Harangi, B., Lazar, I., Hajdu, A.: 'Automatic exudate detection using active contour model and region wise classification'. Conf. Proc. IEEE Eng. Med. Biol. Soc., 2012, pp. 5951–5954

12 Akram, M.U., Tariq, A., Anjum, M.A., Javed, M.Y.: 'Automated detection of exudates in colored retinal images for diagnosis of diabetic retinopathy', *Appl. Opt.*, 2012, **51**, pp. 4858–4866

13 Rocha, A., Carvalho, T., Jelinek, H.F., Goldenstein, S., Wainer, J.: 'Points of interest and visual dictionaries for automatic retinal lesion detection', *IEEE Trans. Biomed. Eng.*, 2012, **59**, (8), pp. 2244–2253

14 Sinthanayothin, C., Boyce, J.F., Cook, H.L., Williamson, T.H.: 'Automated localization of the optic disc, fovea and retinal blood vessels from digital color fundus images', *Br. J. Ophthalmol.*, 1999, **83**, (8), pp. 231–238

15 Osareh, A., Mirmehdi, M., Thomas, B., Markham, R.: 'Automatic recognition of exudative maculopathy using fuzzy c-means clustering and neural networks'. Proc. Med. Image Understand. Anal. Conf., 2001, pp. 49–52

16 Walter, T.: 'Détection de Pathologies Rétiniennes à Partir d'Images Couleur du Fond d'oeil. Rapport d'avancement de thèse'. Ecole des Mines de Paris, Centre de Morphologie Mathématique, Paris, France, 2000

17 Cree, M.J., Olson, J.A., McHardy, K.C., Sharp, P.F., Forrester, J.V.: 'The preprocessing of retinal images for the detection of fluorescein leakage', *Phys. Med. Biol.*, 1999, **44**, (1), pp. 293–308

18 Peli, E., Peli, T.: 'Restoration of retinal images obtained through cataracts', *IEEE Trans. Med. Imaging*, 1989, **8**, (4), pp. 401–406

19 Hsu, W., Pallawa, P.M.D.S., Li Lee, M., Eong, K.-G. A.: 'The role of domain knowledge in the detection of retinal hard exudates'. Proc. of the IEEE Conf. Computer Vision and Pattern Recognition (CVPR), Kauai, Hi, USA, 2001, vol. 2, pp. 246–251

20 Walter, T., Klein, J.-C., Massin, P., Erginay, A.: 'A contribution of image processing to the diagnosis of diabetic retinopathy – detection

doi: 10.1049/iet-ipr.2013.0565

of exudates in color fundus images of the human retina', *IEEE Trans. Med. Imaging*, 2002, **21**, (10), pp. 1236–1243
21 Sánchez, C.I., Hornero, R., López, M.I., Poza, J.: 'Retinal image analysis to detect and quantify lesions associated with diabetic retinopathy'. Conf. Proc. IEEE Eng. Med. Biol. Soc., San Francisco, CA, USA, 2004, pp. 1624–1627
22 Zhang, X., Chutatape, O.: 'Detection and classification of bright lesions in colour fundus images'. Proc. of IEEE Int. Conf. Image Processing, 2004, vol. 1, pp. 139–142
23 Osareh, A., Mirmehdi, M., Thomas, B., Markham, R.: 'Classification and localization of diabetic-related eye disease'. Proc. of Seventh European Conf. on Computer Vision, 2002, pp. 502–516
24 Li, H., Chutatape, O.: 'Automated feature extraction in color retinal images by a model based approach', *IEEE Trans. Biomed. Eng.*, 2004, **51**, (2), pp. 246–254
25 Wang, H., Hsu, W., Goh, K.G., Lee, M.L.: 'An effective approach to detect lesions in color retinal images'. Proc. of the IEEE Conf. on Computer Vision and Pattern Recognition, 2000, pp. 181–186
26 Faust, O., Acharya, U.R., Ng, E.Y., Ng, K.H., Suri, J.S.: 'Algorithms for the automated detection of diabetic retinopathy using digital fundus images: a review', *J. Med. Syst.*, 2012, **36**, pp. 145–157
27 Tariq, A., Akram, M.U., Shaukat, A., Khan, S.A.: 'Automated detection and grading of diabetic maculopathy in digital retinal images', *J. Digit. Imaging*, 2013, **26**, pp. 803–812
28 Youssef, D., Solouma, N.H.: 'Accurate detection of blood vessels improves the detection of exudates in color fundus images', *Comput. Methods Programs Biomed.*, 2012, **108**, pp. 1052–106
29 Jaafar, H.F., Nandi, A.K., Al-Nuaimy, W.: 'Decision support system for the detection and grading of hard exudates from color fundus photographs', *J. Biomed. Opt.*, 2011, **16**, pp. 116001